Downregulation of microRNA-423-5p suppresses TGF-β1-induced EMT by targeting FOXP4 in airway fibrosis

YI CHEN[1], XUAN LI[2], YISHI LI[1], YONGCHANG WU[1], GUICHUAN HUANG[1], XIN WANG[1] and SHULIANG GUO[1]

Departments of [1]Pulmonary and Critical Care Medicine and [2]Clinical Nutrition, The First Affiliated Hospital of Chongqing Medical University, Chongqing 400016, P.R. China

Received October 8, 2021; Accepted March 30, 2022

DOI: 10.3892/mmr.2022.12758

Abstract. Airway fibrosis (AF) is a common disease that can severely affect patient prognosis. Epithelial-mesenchymal transition (EMT) participates in the pathophysiological development of AF and several studies have demonstrated that some microRNAs (miRNAs) contribute to the development of EMT. The aim of this study was to investigate the function of miR-423-5p in the EMT process and its possible underlying mechanism in BEAS-2B cells. The present study utilized the BEAS-2B cell line to model EMT in AF. Online tools, fluorescence *in situ* hybridization analysis and an RNA pull-down assay were used to identify potential target genes of miR-423-5p. In addition, immunohistochemistry, wound healing assays, Transwell migration assays, flow cytometry, enzyme-linked immunosorbent assay, reverse transcription-quantitative PCR, western blot analysis and immunofluorescence staining were used to determine the function of miR-423-5p and its target gene in the EMT process in AF. The results indicated that the miR-423-5p expression in AF tissues and BEAS-2B cells stimulated with 10 ng/ml TGF-β1 for 24 h was significantly increased compared with that in the control group. Overexpression of miR-423-5p facilitated TGF-β1-induced EMT in BEAS-2B cells; by contrast, downregulation of miR-423-5p suppressed TGF-β1-induced EMT in BEAS-2B cells. Furthermore, forkhead box p4 (FOXP4) was identified as a potential target gene of miR-423-5p and changes in the miR-423-5p and FOXP4 expression were shown to significantly affect the expression of PI3K/AKT/mTOR pathway members. In summary, overexpression of miR-423-5P promoted the EMT process in AF by downregulating FOXP4 expression and the underlying mechanism may partly involve activation of the PI3K/AKT/mTOR pathway.

Correspondence to: Dr Shuliang Guo, Department of Pulmonary and Critical Care Medicine, The First Affiliated Hospital of Chongqing Medical University, 1 Youyi Rd, Chongqing 400016, P.R. China
E-mail: guosl999@sina.com

Abbreviations: AF, airway fibrosis; FOXP4, forkhead box p4; miR, microRNA; α-SMA, α-smooth muscle actin; H&E, hematoxylin and eosin; ELISA, enzyme-linked immunosorbent assay; FISH, fluorescence *in situ* hybridization.

Key words: microRNA-423-5p, airway fibrosis, forkhead box p4, epithelial-mesenchymal transition, PI3K/AKT/mTOR signaling pathway

Introduction

Airway fibrosis (AF) is a common, chronic and progressive disease with an unclear etiology (1). AF can be caused by several pathogenic factors and is characterized by repetitive airway epithelial cell injury, fibroblast activation and increased extracellular matrix deposition, resulting in airway destruction (2). Despite the development of various detection methods and clinical treatments, the morbidity and mortality of AF remain high and AF remains a serious threat to public health (3). Therefore, the need to determine the underlying mechanism of AF is urgent.

Several studies have suggested that one possible pathogenesis mechanism of AF involves epithelial-mesenchymal transition (EMT), which is defined by the loss of epithelial features and the gain of mesenchymal features (4,5); therefore, EMT serves an important role in fibrosis pathology (6). Increasing evidence indicates that TGF-β1 is a master switch for the induction of fibrosis in various organs (7). TGF-β1 can upregulate profibrotic gene expression, such as N-cadherin, vimentin and α-smooth muscle actin (α-SMA); and simultaneously downregulate the expression of epithelial cell-related genes, such as E-cadherin, promoting AF (8).

MicroRNAs (miRNAs or miRs) are a class of small, noncoding RNAs that inhibit gene expression by binding target gene 3'-untranslated regions (3'-UTRs) (9). Increasing evidence shows that miRNAs participate in various biological processes, including cell proliferation, differentiation and apoptosis (10). Additionally, accumulated evidence indicates that miRNAs are vital to the EMT process in AF (11). For example, Li *et al* (12) found that 'miR-184 targets TP63 to block idiopathic pulmonary fibrosis by inhibiting proliferation and epithelial-mesenchymal transition of airway epithelial cells'. Moreover, the miRNA miR-423-5p is known to be involved in the regulation of the EMT process in various diseases (13). Nevertheless, to the best of the authors' knowledge, the possible role of miR-423-5p in AF development has not been studied.

The aim of the present study was to detect miR-423-5p expression in normal airway tissue and AF tissue. In addition, the role of miR-423-5p in TGF-β1-induced EMT was determined in the BEAS-2B cell line. Finally, the underlying mechanism by which miR-423-5p affects TGF-β1-induced EMT was examined.

Materials and methods

Ethics statement. The First Affiliated Hospital of Chongqing Medical University Ethics Committee approved the present study (institutional approval number. 2020-147) and the research was performed in accordance with the Declaration of Helsinki; all subjects provided written informed consent.

Tissues, cells and cell culture. A total of 10 AF tissue samples were collected from patients undergoing fiberoptic bronchoscopy biopsy (7 females and 3 males). The scar tissue samples were collected from patients undergoing fiberoptic bronchoscopy biopsy via an electrocautery needle knife (VIO 300S; Erbe Elektromedizin GmbH). A total of 10 control airway tissue samples (from 4 females and 6 males) were obtained from normal areas of the central airway removed during nasopharyngeal cancer resection. The 64-slice helical high-resolution computed tomography (HRCT) system (Siemens AG) was used to obtain HRCT chest images and two radiologists blinded on clinical data interpreting all HRCT findings by consensus. Tracheal stenosis and bronchomalacia were diagnosed based on lesions detection by a bronchoscope (CV-290; Olympus Corporation). Detailed information on the control subjects and AF patients who were diagnosed with AF by pathology examination is provided in Table I. The inclusion criteria for control subjects were as follows: nasopharyngeal cancer resection and the absence of other airway diseases. From the included subjects, normal areas of the central airway were collected. All tissue samples were collected between June 2020 and December 2020 at The First Affiliated Hospital of Chongqing Medical University. Human airway epithelial cells (BEAS-2B) were purchased from the Cell Bank of the Chinese Academy of Sciences. The cells were maintained in DMEM/F12 medium (Gibco; Thermo Fisher Scientific, Inc.) containing 10% FBS (PAN-Biotech GmbH), 100 U/ml penicillin and 100 μg/ml streptomycin at 37˚C in a humidified 5% CO_2 atmosphere. BEAS-2B cells were treated with 10 ng/ml TGF-β1 (PeproTech, Inc.) at 37˚C for 24 h to establish the EMT cell model as previously described (8).

Cell transfection. BEAS-2B cells were transfected with a miR-423-5p mimic or inhibitor (Shanghai GenePharma Co, Ltd.) at a final concentration of 50 nM and FOXP4 short interfering (si)RNA (Guangzhou RiboBio Co., Ltd.) or negative control (NC) siRNA using Lipofectamine® 3000 (Invitrogen; Thermo Fisher Scientific, Inc.). The sequences of the miR-423-5p mimic and inhibitor, the corresponding NCs, FOXP4 siRNA and NC siRNA are provided in Table II. After 24 h of transfection, the cells were treated with or without 10 ng/ml TGF-β1 for 24 h at 37˚C and then collected for further experiments.

Histological analysis. Tissue sections (5 μm thick) were subjected to hematoxylin and eosin (H&E) and Masson staining to enable histological evaluation of airway tissue fibrosis. Paraffin embedding was used following dehydration with 70 and 90% alcohol then transparency with xylene and permeation with paraffin. Finally, Hematoxylin was used for 1 min and eosin for 2 min at room temperature to stain the slices. Furthermore, Masson staining was performed for 3 min at room temperature.

Immunohistochemistry. Paraffin-embedded airway tissue sections were dewaxed in xylene, dehydrated in graded alcohol and incubated in 3% H_2O_2 for 0.5 h. The tissue sections were then blocked with normal goat serum (Wuhan Servicebio Technology Co., Ltd.) and incubated with anti-TGF-β1 (1:100; Wuhan Servicebio Technology Co., Ltd. cat. no. GB13028), anti-E-cadherin (1:200; Wuhan Servicebio Technology Co., Ltd. cat. no. GB12082), anti-N-cadherin (1:100; Wuhan Servicebio Technology Co., Ltd. cat. no. GB13447), anti-α-SMA (1:500; Wuhan Servicebio Technology Co., Ltd. cat. no. GB111364), anti-vimentin (1:500; Wuhan Servicebio Technology Co., Ltd. cat. no. GB111308), anti-FOXP4 (1:200; ProteinTech, Wuhan, China; cat. no. 16772-1-AP), anti-PI3K (1:1,000; Wuhan Servicebio Technology Co., Ltd. no.GB113360), anti-Akt (1:500; Wuhan Servicebio Technology Co., Ltd. cat. no. GB11629) and anti-mTOR (1:200; Wuhan Servicebio Technology Co., Ltd. cat. no. GB111839) antibodies overnight at 4˚C. After incubation with an HRP-labelled secondary antibody (goat-anti rabbit IgG) for 2 h in room temperature, the sections were observed under a light microscope (Nikon Eclipse 80i; Nikon Corporation).

Wound healing assay. BEAS-2B cells were seeded into a six-well plate and transfected as described above. A 10-μl pipette tip was used to scrape the cell monolayer, after which the cells were washed three times with PBS to remove cellular debris and floating cells. Then, 1.000 μl of serum-free medium containing 10 ng/ml TGF-β1 or the equivalent amount of PBS was added, the migration ability was measured by capturing the images at the beginning and in the same position after 24 h.

Transwell migration assay. Transwell inserts (pore size: 8.0 μm; Corning, Inc.) were used for the migration assay. The ability of the various groups of cells to migrate was detected according to the manufacturer's instructions.

Flow cytometry. Cellular apoptosis was performed by flow cytometry (CytoFLEX; Beckman Coulter, Brea) using an Annexin V-FITC/Propidium Iodine double staining kit (Tianjin Sungene Biotech Co., Ltd.) according to manufacturer's instructions. Cells ($1x10^6$) were stained for 15 min at room temperature in the dark. After washing twice, the cells were resuspended in 200 μl PBS and analyzed using a FACSCalibur flow cytometer (BD Biosciences). The apoptotic rate was calculated by counting early and late apoptotic cells percentage.

ELISA. Culture medium was collected from each group and centrifuged at 3,000 x g for 10 min at 4˚C, after which the supernatant was collected for further examination. The levels of FOXP4, E-cadherin, N-cadherin, vimentin and α-SMA were detected using ELISA kits (Meike Jiangsu Sumeike

Table I. Clinical features of patients and controls.

Number	Type	Age (years)	Sex	Smoking	Cough	Dyspnoea	Wheezing	Atelectasis (chest HRCT features)	Tracheal stenosis (Bronchoscopic features)	Bronchomalacia (Bronchoscopic features)	Diagnose
1	AF	38	Female	No	Yes	No	No	Yes	No	Yes	TBTB
2	AF	40	Male	Yes	Yes	No	No	No	No	Yes	TBTB
3	AF	44	Female	No	Yes	No	Yes	No	No	Yes	TBTB
4	AF	34	Female	No	Yes	Yes	No	No	Yes	Yes	TBTB
5	AF	47	Female	Yes	No	Yes	No	Yes	No	No	TBTB
6	AF	34	Male	No	Yes	No	Yes	No	Yes	No	TBTB
7	AF	37	Female	No	No	Yes	No	No	No	No	TBTB
8	AF	41	Female	No	Yes	No	No	No	No	No	TBTB
9	AF	46	Female	No	Yes	Yes	No	No	No	No	TBTB
10	AF	31	Male	Yes	Yes	Yes	No	No	No	Yes	TBTB
11	Control	51	Male	Yes	No	No	No	No	No	No	NPC
12	Control	63	Female	No	No	Yes	No	No	No	No	NPC
13	Control	62	Male	Yes	Yes	No	Yes	No	No	No	NPC
14	Control	58	Female	No	Yes	Yes	No	Yes	No	No	NPC
15	Control	47	Male	Yes	No	No	No	No	No	No	NPC
16	Control	50	Female	No	No	No	No	No	No	No	NPC
17	Control	48	Female	No	No	Yes	No	No	No	No	NPC
18	Control	49	Male	Yes	Yes	No	No	No	No	No	NPC
19	Control	55	Male	No	No	Yes	No	No	No	No	NPC
20	Control	52	Female	Yes	No	No	No	No	No	No	NPC

AF, airway fibrosis; TBTB, Tracheobronchial tuberculosis; NPC, nasopharyngeal cancer.

Table II. Sequences of miR-423-5p mimic, inhibitor, NC, FOXP4 siRNA and siRNA NC.

Gene	Sense	Antisense
hsa-miR-423-5p mimics	UGAGGGGCAGAGAGCGAGACUUU	AGUCUCGCUCUCUGCCCCUCAUU
hsa-miR-423-5p inhibitor	AAAGUCUCGCUCUCUGCCCCUCA	
Mimic NC	UUCUCCGAACGUGUCACGUTT	ACGUGACACGUUCGGAGAATT
Inhibitor NC	CAGUACUUUUGUGUAGUACAA	
genOFFTM st-h-FOXP4_001		CCTCAGCTATGGAGCACTT
genOFFTM st-h-FOXP4_002		GCAGACAGCAATGGTGAGA
genOFFTM st-h-FOXP4_003		TTCGCCTATTTCCGCAGAA
NC-siRNA		GGCUCUAGAAAAGCCUAUGCdTdT

miR, microRNA; NC, corresponding negative control; FOXP4, Forkhead box p4; si, short interfering; d, deoxyribonucleoside.

Biological Technology Co., Ltd.) according to the manufacturer's instructions. At least three parallel wells were analyzed for each sample.

Reverse transcription-quantitative (RT-q) PCR. Total RNA (1 μg) from airway tissues or BEAS-2B cells (1x10^6) was used to synthesize complementary DNA (cDNA) with the PrimeScript RT Reagent kit (Takara Biotechnology Co., Ltd.). Subsequently, cDNA was amplified via the TB Green Premix EX Taq II PCR kit (Takara Biotechnology Co., Ltd.). Amplification cycle included an initial 30 sec incubation at 95˚C for denaturation, followed by 40 cycles of 5 sec at 95˚C for annealing and 30 sec at 60˚C for elongation. The small nuclear RNA U6 was utilized for the internal normalization of miR-423-5p levels and GAPDH was utilized as a control for mRNA expression. Relative quantification was carried out via the $2^{-\Delta\Delta Cq}$ method (14). The primer sequences used are listed in Table SI. RNA extraction, cDNA synthesis and qPCR were

performed according to the manufacturer's protocols and these experiments were replicated three times.

Western blot assay. Total protein was extracted from the BEAS-2B cells using RIPA lysis buffer (Beyotime Institute of Biotechnology) mixing with protease and phosphatase inhibitor. The proteins were quantified by bicinchoninic acid kit (Beyotime Institute of Biotechnology). Proteins (25 μg) extracted from BEAS-2B cells were separated via 10% SDS-PAGE and transferred onto PVDF membranes (EMD Millipore). The membranes were blocked with 5% nonfat milk at room temperature for 2 h and then incubated overnight with specific primary antibodies at 4˚C. The next day, the membranes were washed three times with Tris-buffered saline containing 1% Tween-20 and then incubated with secondary antibodies (1:8,000; Zhongshan Golden Bridge Biological Technology Co., Ltd.; cat. no. ZB-2306) for 1 h at room temperature. The following primary antibodies were utilized: anti-E-cadherin (1:10,000; Abcam; cat. no. ab40772), anti-N-cadherin (1:1,000; CST; cat. no. 13116T), anti-α-SMA (1:2,000; Abcam; cat. no. ab32575), anti-vimentin (1:3,000; Abcam; cat. no. ab92547), anti-FOXP4 (1:600; Affinity; cat. no. AF4057), anti-phosphorylated (p)-PI3K (1:800; Affinity; cat. no. AF3241), anti-PI3K (1:1,000; CST; cat. no. 4257T), anti-p-Akt (1:800; CST; cat. no. 4060T), anti-Akt (1:1,000; CST; cat. no. 4691T), anti-p-mTOR (1:1,000; CST; cat. no. 5536T), anti-mTOR (1:1,000; CST; cat. no. 2983T) and anti-β-actin (1:2,000; Chongqing Biospes Co., Ltd.; cat. no. BTL1026). The western blots results were analyzed by Bio-Rad gel imaging system (170-8170, Bio-Rad Laboratories, Inc.) and western blot kit (Beyotime Institute of Biotechnology).

Immunofluorescence staining. Precooled PBS was used to rinse BEAS-2B cells three times for 5 min each and then the cells were fixed with 4% paraformaldehyde for 20 min at room temperature. Goat serum was used to block the cells for 1 h at 37˚C. The BEAS-2B cells were incubated with primary antibodies against E-cadherin (1:200; CST), N-cadherin (1:200; CST), vimentin (1:200; CST), α-SMA (1:200; CST) and FOXP4 (1:200; ProteinTech Group, Inc.) at 4˚C overnight in a wet box, rinsed with precooled PBS three times, incubated with donkey anti-rabbit IgG (Alexa Fluor 64) (1:500; Abcam, USA) for 1 h in the dark at 37˚C and then rinsed three times with PBS. The BEAS-2B cells were then treated with DAPI for 20 min at 4˚C in the dark to stain the cell nuclei.

RNA fluorescence in situ hybridization (FISH) analysis. The Ribo FISH kit (Guangzhou RiboBio Co., Ltd.) was used for FISH experiments. In brief, BEAS-2B cells were cultured to 60% confluence prior to the experiments. Prechilled permeate at 4˚C for 5 min and 4% paraformaldehyde at room temperature for 10 min were used for cell permeation and fixation, respectively. Fixed cells were incubated with a FISH Probe Mix stock solution. Nuclei were stained with DAPI for 20 min at 4˚C in the dark.

RNA pull-down assay. A potential target gene of miR-423-5p was identified using TargetScan (version 7.2; http://www.targetscan.org/). The FOXP4 and FOXP4-NC sequences were labelled with biotin by Shanghai GenePharma Co., Ltd. The biotinylated oligonucleotides were transfected into BEAS-2B cells at 4˚C for 24 h and the cells were lysed with RIP lysis buffer (MilliporeSigma), followed by incubation with Streptavidin MagneSphere magnetic beads (MilliporeSigma) at room temperature for 3 h. The magnetic beads were washed and the RNA and mRNA sequences pulled down by the antibodies were assessed by RT-qPCR.

Statistical analyses. The data were analyzed via SPSS 23.0 software (IBM Corp.) and are presented as the mean ± SD (n=3). Comparisons between two groups were carried out via unpaired Student's t-tests. Multiple comparisons were carried out via one-way ANOVA followed by the homogeneity test of variance and then Tukey's post hoc test was performed. $P<0.05$ was considered to indicate a statistically significant difference.

Results

miR-423-5p is upregulated in AF tissues and TGF-β1-treated BEAS-2B cells. The principal histological findings based on the H&E and Masson staining results were squamous epithelialization of the bronchial epithelial cells and fibrotic lesions with thickened submucosal layers. In addition, the fibrosis presence was verified by Masson staining (Fig. 1A). To investigate whether miR-423-5p participates in EMT development, miR-423-5p expression in AF tissue and during TGF-β1-induced EMT was detected. The expression of miR-423-5p, TGF-β1, N-cadherin, vimentin and α-SMA was significantly increased in AF tissue compared with control tissue; conversely, E-cadherin expression was decreased (Figs. 1B, C, E and F and S1A). miR-423-5p expression in BEAS-2B cells treated with TGF-β1 was then detected, which showed that TGF-β1 upregulated miR-423-5p expression compared with that in the control group (Fig. 1D). Taken together, these findings indicated that miR-423-5p expression was upregulated in both AF tissues and TGF-β1-stimulated BEAS-2B cells.

miR-423-5p promotes TGF-β1-induced EMT. To assess the role of miR-423-5p in TGF-β1-induced EMT in BEAS-2B cells, a miR-423-5p mimic or inhibitor was transfected into BEAS-2B cells, which were then treated with TGF-β1. The miRNA transfection efficiency was verified using RT-qPCR. After 24 h of transfection, the miR-423-5p level increased by ~20-fold in the miR-423-5p mimic group compared with the mimic-NC group. Additionally, the miR-423-5p level decreased by ~6-fold in the miR-423-5p inhibitor group compared with the inhibitor-NC group (Fig. S1B). These results demonstrated that the transfection was efficient. To reveal the functional effect of miR-423-5p on the BEAS-2B cell model of EMT induced by TGF-β1, the EMT biomarkers E-cadherin, N-cadherin, vimentin and α-SMA were detected via RT-qPCR, immunofluorescence staining, ELISA and western blot analysis. In addition, a wound healing assay and Transwell migration assay were used to examine the ability of the cells to migrate. Furthermore, the apoptosis of BEAS-2B cells was determined by flow cytometry. The results showed that upregulation of miR-423-5p decreased

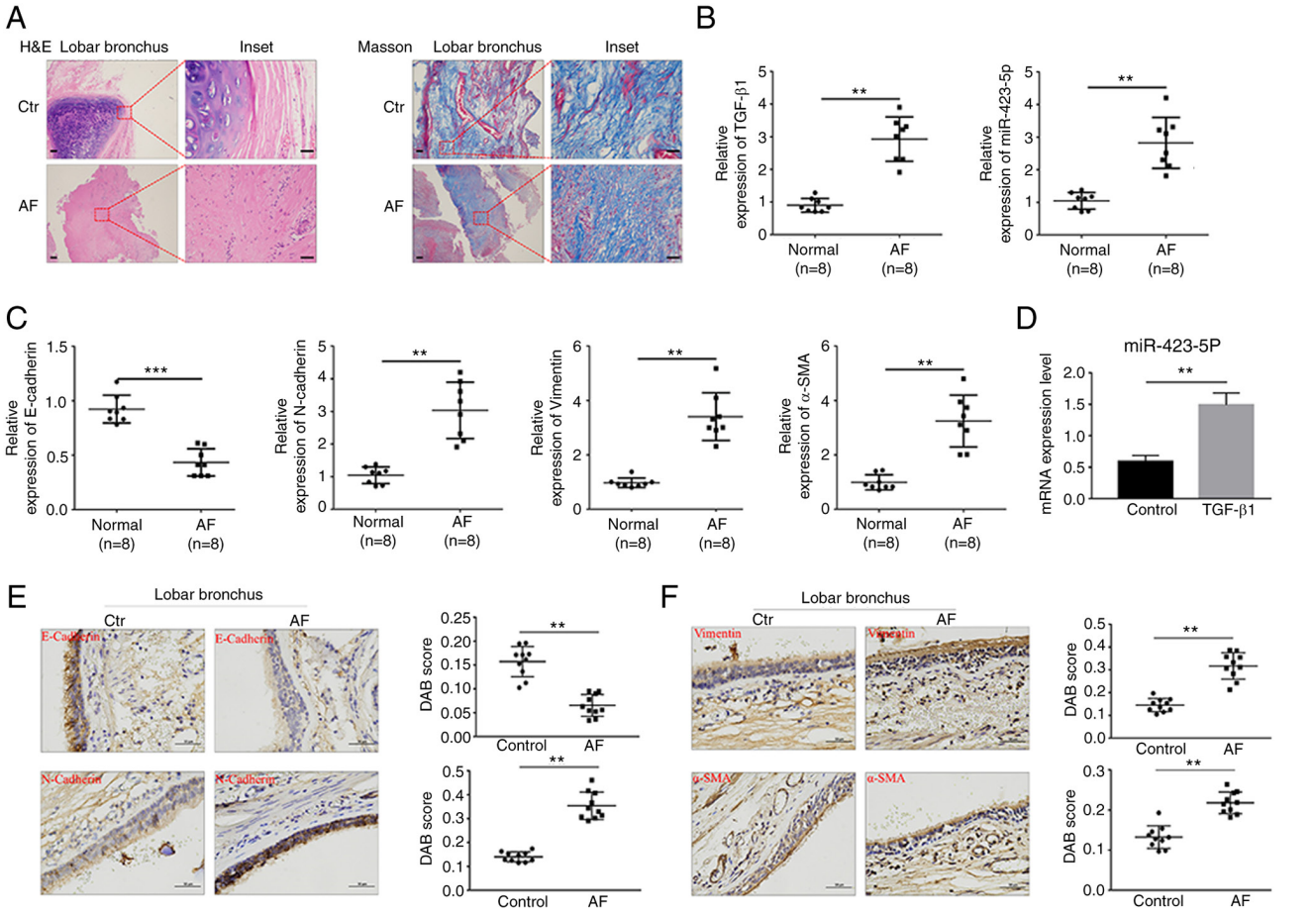

Figure 1. miR-423-5p expression in human AF tissue and BEAS-2B cells treated with TGF-β1. (A) H&E and Masson staining of the control group and AF group. Scale bar=500 and 100 μm (inset) respectively. (B and C) The relative expression of TGF-β1, miR-423-5p, E-cadherin, N-cadherin, vimentin and α-SMA in normal airway tissues (n=8) and AF tissues (n=8) was determined by RT-qPCR. (D) The relative expression of miR-423-5p in BEAS-2B cells treated with 10 ng/ml TGF-β1 for 24 h was determined by RT-qPCR. (E and F) The protein expression of E-cadherin, N-cadherin, vimentin and α-SMA in normal airway tissues (n=10) and AF tissues (n=10) was detected by immunohistochemistry. Scale bar=50 μm. **P<0.01 and ***P<0.001. miR, microRNA; AF, airway fibrosis; H&E, hematoxylin and eosin; α-SMA, α-smooth muscle actin; RT-qPCR, reverse transcription-quantitative PCR; Ctr, control.

TGF-β1-stimulated E-cadherin expression but increased the expression of N-cadherin, vimentin and α-SMA at both the mRNA and protein levels. In contrast, downregulation of miR-423-5p increased TGF-β1-stimulated E-cadherin expression but decreased N-cadherin, vimentin and α-SMA expression at both the mRNA and protein levels (Fig. 2A-D). Additionally, miR-423-5p upregulation increased BEAS-2B cell migration and suppressed BEAS-2B cell apoptosis. In contrast, miR-423-5p downregulation decreased the migration of BEAS-2B cells and promoted BEAS-2B cell apoptosis (Figs. 2E and F and S1C). Collectively, these findings suggested that upregulation of miR-423-5p promoted TGF-β1-induced EMT, whereas downregulation of miR-423-5p suppressed TGF-β1-induced EMT.

FOXP4 is a target gene of miR-423-5p. Target genes of miR-423-5p were predicted via the online database TargetScan 7.2 and the results identified FOXP4 (Fig. S1D). To confirm FOXP4 as a miR-423-5p target gene, RNA FISH analysis and an RNA pull-down assay were performed. The results of FISH analysis indicated that miR-423-5p was located in the cytoplasm or nucleus and that FOXP4 mRNA was located in the nucleus. The results also revealed the colocalization of miR-423-5p and FOXP4 mRNAs in the nuclei of BEAS-2B cells, suggesting an interaction between them (Fig. 3A-C). FOXP4 mRNA expression in the input-FOXP4 group was higher than that in the input-NC groups, showing that the FOXP4 gene was bound by the probe. Moreover, miR-423-5p expression in the input-FOXP4 group was higher than that in the input-NC group, indicating that miR-423-5p and FOXP4 were bound (Fig. 3D). Furthermore, FOXP4 expression was detected in AF tissues and TGF-β1-treated BEAS-2B cells. The results showed that FOXP4 expression was clearly decreased in the AF tissues and BEAS-2B cells treated with TGF-β1 at both the mRNA and protein levels (Figs. 3E and S1E). In addition, the association between miR-423-5p and FOXP4 was detected by RT-qPCR, immunofluorescence staining and western blot analysis. FOXP4 expression was decreased in the miR-423-5p mimic group compared with the mimic-NC group at both the mRNA and protein levels but increased in the miR-423-5p inhibitor group compared with the inhibitor-NC group, indicating a negative association between miR-423-5p and FOXP4 (Fig. 3F-H). These findings suggested that FOXP4 is directly regulated by miR-423-5p.

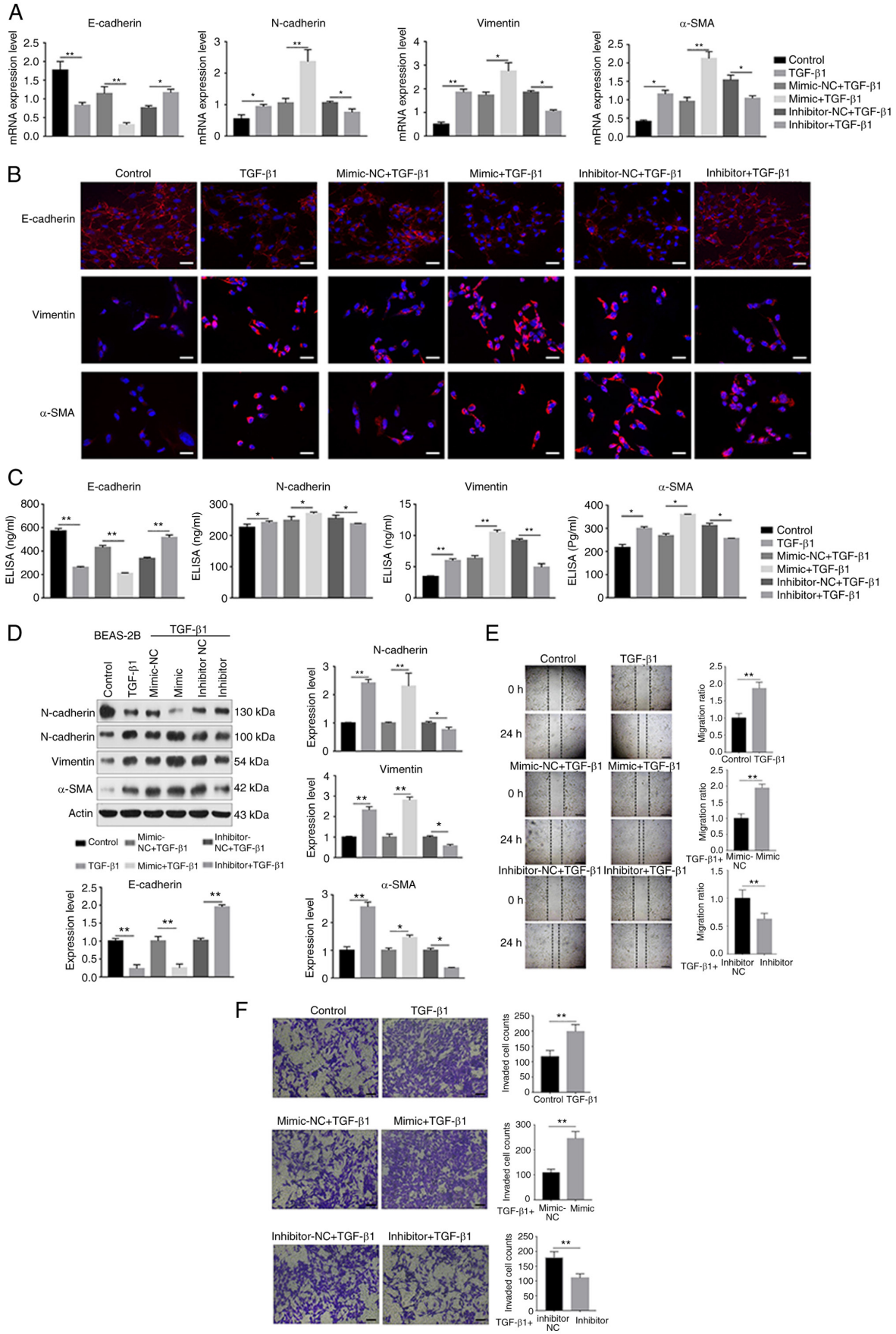

Figure 2. Effect of miR-423-5p on TGF-β1-induced EMT. The relative expression of E-cadherin, N-cadherin, vimentin and α-SMA in BEAS-2B cells transfected with a miR-423-5p mimic or inhibitor for 24 h and then treated with TGF-β1 for 24 h was determined by (A) Reverse transcription-quantitative PCR and (B) immunofluorescence staining (scale bar=50 μm.), (C) ELISA and (D) western blot analysis. The ability of BEAS-2B cells transfected with a miR-423-5p mimic or inhibitor for 24 h and then treated with TGF-β1 for 24 h to migrate was detected by a (E) wound healing assay (scale bar=200 μm.) and (F) Transwell migration assay (Scale bar=100 μm.). *P<0.05 and **P<0.01. miR, microRNA; EMT, epithelial-mesenchymal transition; α-SMA, α-smooth muscle actin.

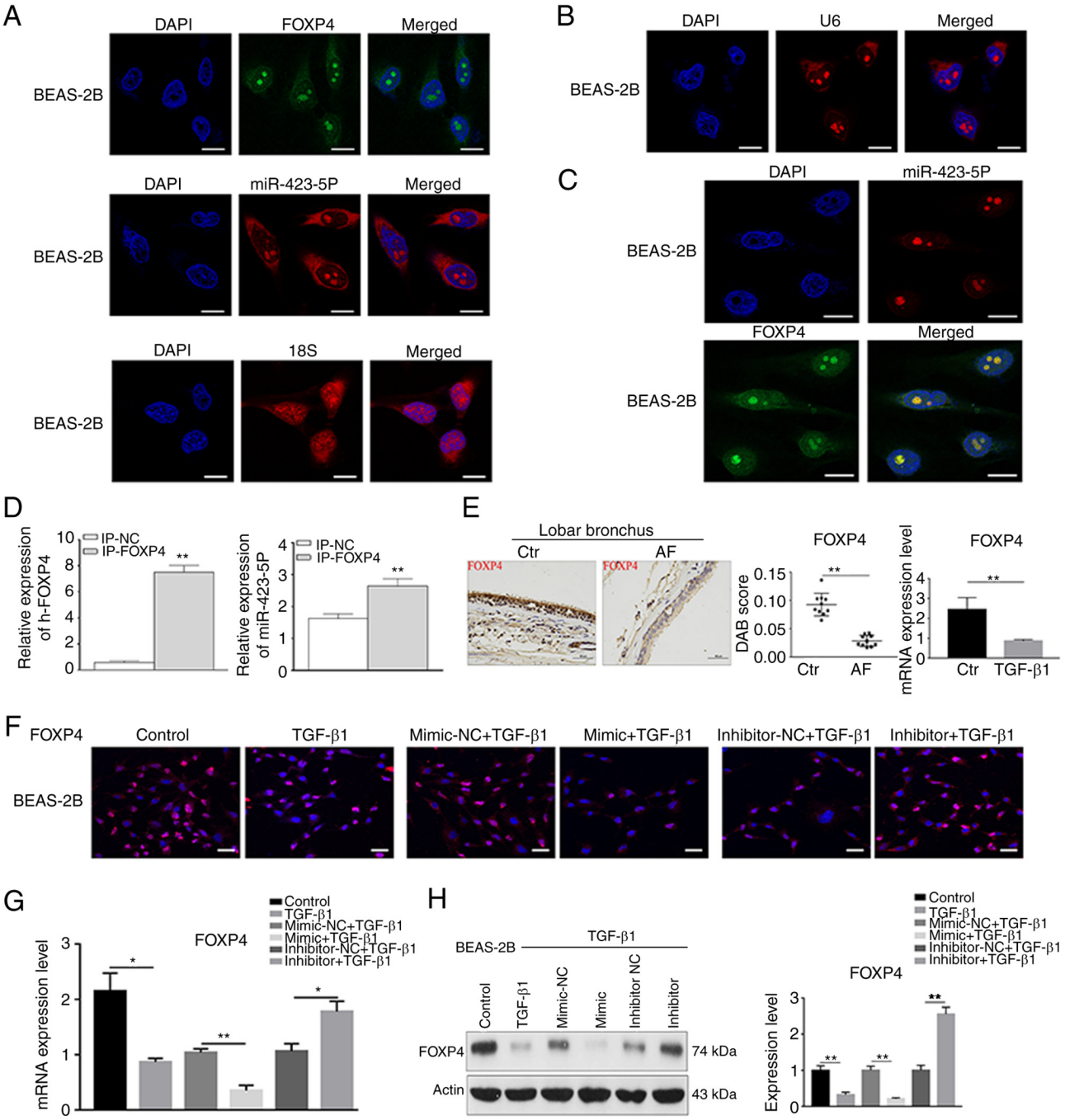

Figure 3. Identification of target genes of miR-423-5p. (A-C) The location of miR-423-5p and FOXP4 mRNA in BEAS-2B cells was determined by fluorescence *in situ* hybridization (scale bar=200 μm). (D) The binding of miR-423-5p and FOXP4 in BEAS-2B cells was detected by an RNA pull-down assay. (E) The expression of FOXP4 in AF tissues and TGF-β1-stimulated BEAS-2B cells was detected by immunohistochemistry (scale bar=50 μm) and RT-qPCR. The relative expression of FOXP4 in BEAS-2B cells transfected with a miR-423-5p mimic or inhibitor for 24 h and then treated with TGF-β1 for 24 h was determined by (G) RT-qPCR, (F) immunofluorescence staining (scale bar=50 μm.) and (H) western blot analysis. *P<0.05 and **P<0.01. miR, microRNA; FOXP4, forkhead box p4; RT-qPCR, reverse transcription-quantitative PCR; AF, airway fibrosis.

FOXP4 silencing eliminates miR-423-5p inhibitor-induced effects on TGF-β1-induced EMT. To confirm that the miR-423-5p inhibitor suppressed TGF-β1-induced EMT through a FOXP4-dependent pathway, the miR-423-5p inhibitor was transfected into BEAS-2B cells in which FOXP4 had been knocked down. First, the knockdown efficiency in BEAS-2B cells was tested. The FOXP4 expression was significantly downregulated in the siRNA-FOXP4 group compared with the siRNA-NC group at both the mRNA and protein levels, which demonstrated efficient knockdown (Fig. S1F-H). The results of RT-qPCR, immunofluorescence staining, ELISA and western blot analysis indicated that FOXP4 and E-cadherin expression was decreased, but N-cadherin, vimentin and α-SMA expression was increased in the TGF-β1 + miR-423-5p inhibitor + siRNA-FOXP4 group compared with the TGF-β1 + miR-423-5p inhibitor + siRNA-NC group (Fig. 4A-D). Additionally, the ability of the cells to migrate was increased and apoptosis was decreased in the TGF-β1 + miR-423-5p

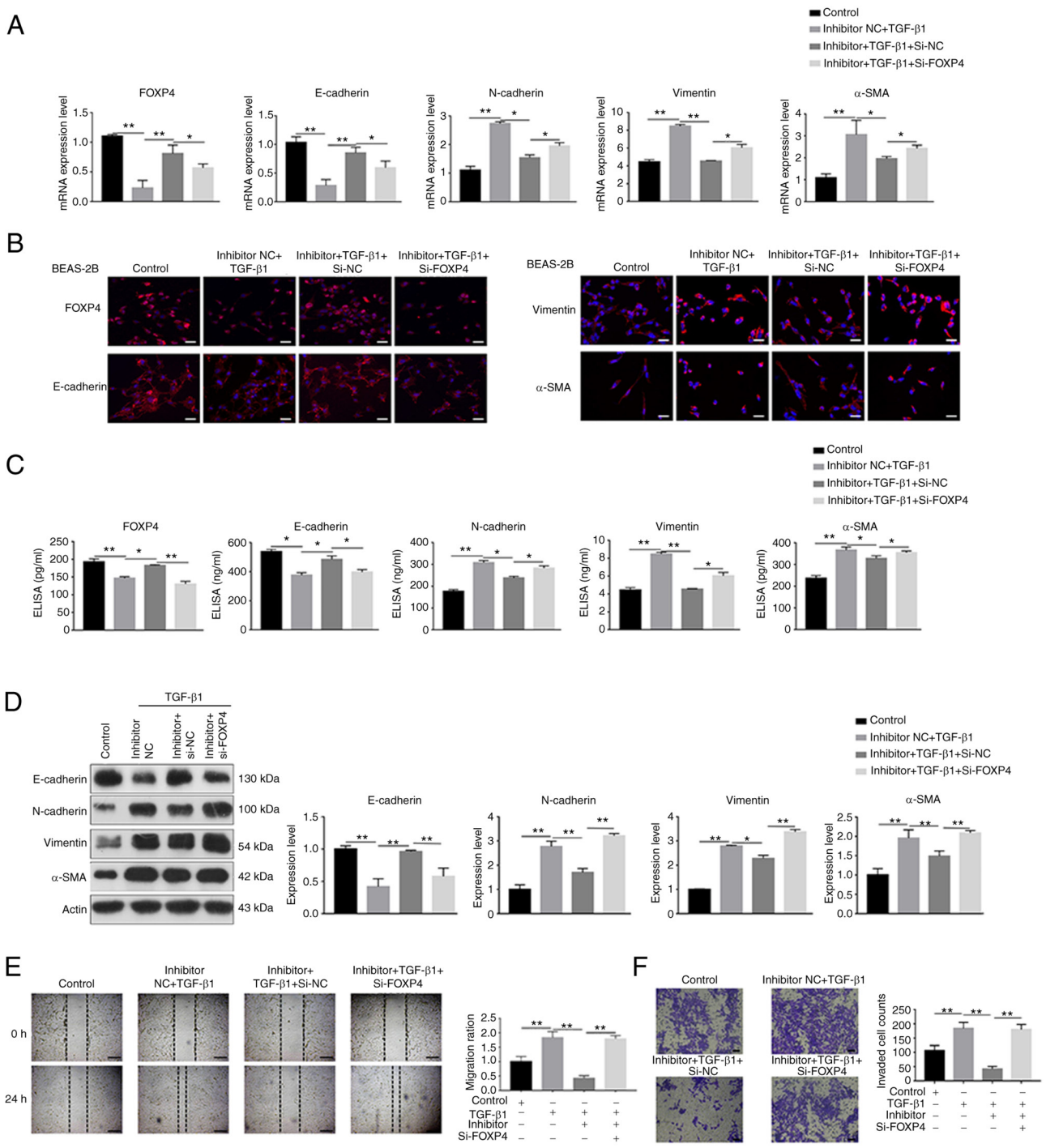

Figure 4. FOXP4 silencing eliminated the miR-423-5p inhibitor-mediated effect on TGF-β1-induced EMT. BEAS-2B cells transfected with siRNA-FOXP4 to silence FOXP4 were transfected with a miR-423-5p inhibitor for 24 h and then treated with TGF-β1 for 24 h. The relative expression of FOXP4, E-cadherin, N-cadherin, vimentin and α-SMA was determined by (A) reverse transcription-quantitative PCR, (B) immunofluorescence staining (scale bar=50 μm), (C) ELISA and (D) western blot analysis. Migration and the apoptosis rate were detected by (E) wound healing assay (scale bar=200 μm) and (F) Transwell migration assay (scale bar=100 μm). *P<0.05 and **P<0.01. FOXP4, forkhead box p4; miR, microRNA; EMT, epithelial-mesenchymal transition; si, short interfering; α-SMA, α-smooth muscle actin.

inhibitor + siRNA-FOXP4 group compared with the TGF-β1 + miR-423-5p inhibitor + siRNA-NC group (Figs. 4E and F and S1I). These findings indicated that FOXP4 knockdown partly eliminated miR-423-5p inhibitor-mediated effects on EMT induced by TGF-β1.

miR-423-5p promotes EMT through the PI3K/AKT/mTOR signaling pathway. To reveal the underlying mechanism by which the miR-423-5p mimic promoted TGF-β1-induced EMT, the signaling pathway downstream of FOXP4 was detected. Existing evidence shows that the PI3K/AKT/mTOR pathway participates in the lung fibrosis process; however, the role of the PI3K/AKT/mTOR pathway in the airway is unclear. Therefore, the expression levels of PI3K/AKT/mTOR pathway-associated indicators were evaluated. The expression of PI3K, AKT and mTOR was significantly higher in the AF group than in the

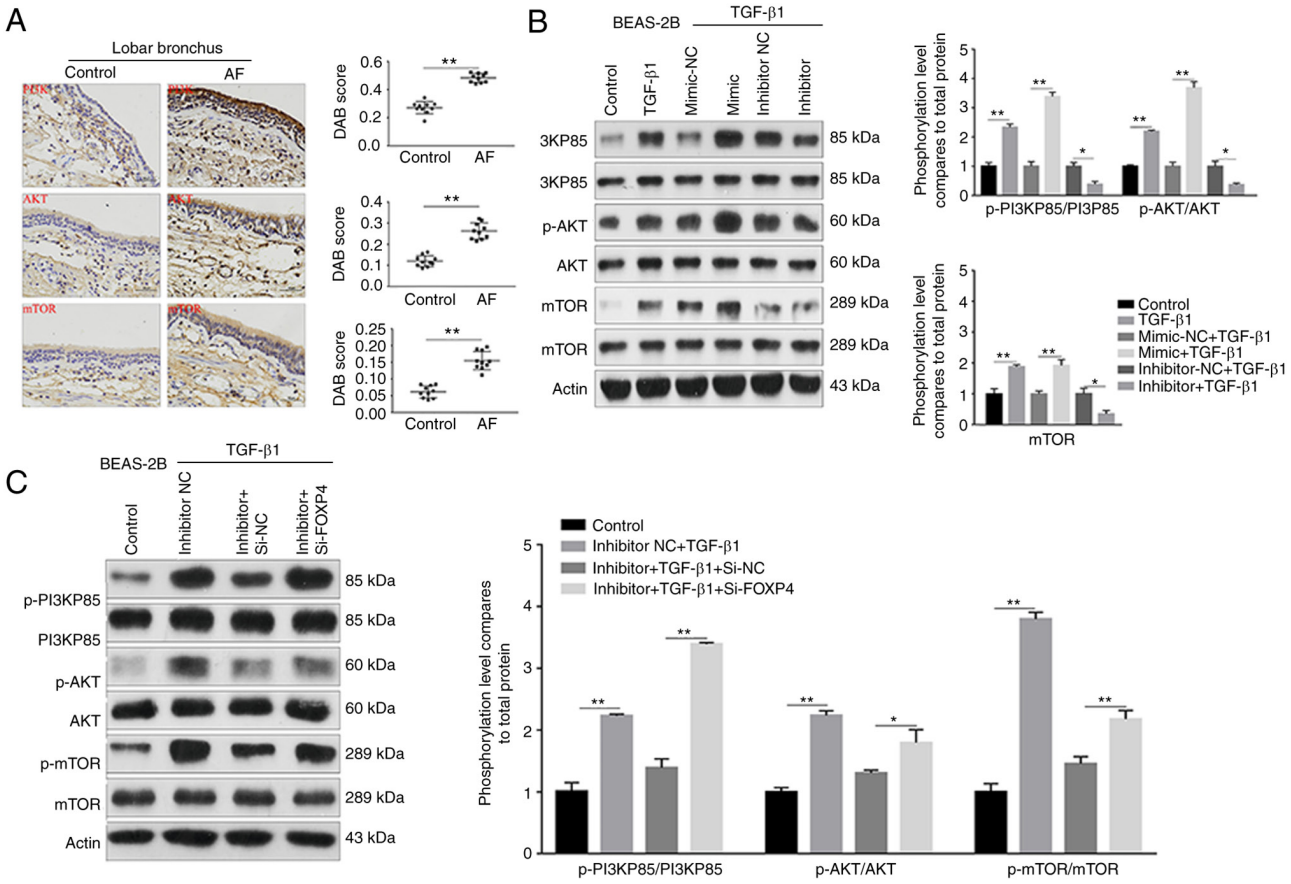

Figure 5. miR-423-5p promotes TGF-β1-induced EMT through the PI3K/AKT/mTOR signaling pathway. (A) The protein expression of PI3K, AKT and mTOR was detected by immunohistochemistry (scale bar=50 μm.). (B) The relative expression of p-PI3K, p-AKT and p-mTOR in BEAS-2B cells transfected with a miR-423-5p mimic or inhibitor for 24 h and then treated with TGF-β1 for 24 h was determined by western blot analysis. (C) The relative expression of p-PI3K, p-AKT and p-mTOR was determined by western blot analysis. BEAS-2B cells transfected with siRNA-FOXP4 to silence FOXP4 were transfected with a miR-423-5p inhibitor for 24 h and then treated with TGF-β1 for 24 h. *P<0.05 and **P<0.01. miR, microRNA; EMT, epithelial-mesenchymal transition; p-, phosphorylated; si, short interfering.

control group (Fig. 5A). Moreover, p-PI3K, p-AKT and p-mTOR expression was significantly increased in the TGF-β1 group compared with the control group. Conversely, in the TGF-β1 + miR-423-5p inhibitor + siRNA-NC group, the expression levels of p-PI3K, p-AKT and p-mTOR were lower than those in the TGF-β1 group (Fig. 5B). Additionally, p-PI3K, p-AKT and p-mTOR expression was clearly upregulated in the TGF-β1 + miR-423-5p inhibitor + siRNA-FOXP4 group compared with the TGF-β1 + miR-423-5p inhibitor + siRNA-NC group (Fig. 5C). Taken together, these findings suggested that miR-423-5p promotes TGF-β1-induced EMT through the PI3K/AKT/mTOR signaling pathway in AF.

Discussion

AF is a progressive airway disease characterized by airway epithelial injury, fibroblast activation and extracellular matrix deposition (15,16). miRNAs are endogenous, small noncoding RNAs that modulate genes at the posttranscriptional level in various physiological and pathological processes (17). Accumulating evidence indicates that miRNAs trigger the onset and progression of AF (18,19).

In the present study, miR-423-5p was found to be upregulated in human AF tissue; additionally, the functional role of miR-423-5p and the underlying mechanism of its effect on AF were identified. The results collected from BEAS-2B cells demonstrated that TGF-β1 increased the expression of miR-423-5p and decreased FOXP4 expression. Additionally, overexpression of miR-423-5p facilitated TGF-β1-induced EMT in BEAS-2B cells; by contrast, downregulation of miR-423-5p suppressed TGF-β1-induced EMT in BEAS-2B cells. In addition, FOXP4 silencing eliminated the miR-423-5p inhibitor-mediated effect on TGF-β1-induced EMT. These results verified that FOXP4 is a potential target of miR-423-5p. EMT serves a critical role in organ fibrosis, including liver and kidney fibrosis (20,21). Moreover, TGF-β1 is an important cytokine involved in the initiation of EMT (22). As AF progresses, alveolar epithelial cell features are gradually replaced by mesenchymal cell features with the development of EMT (23). BEAS-2B cells are an airway alveolar epithelial cell type that shows the general characteristics of alveolar epithelial cells (24), such as a common morphology and specific biomarkers, and this cell line has been used to investigate the mechanisms of EMT in other airway diseases (25,26). Therefore, the BEAS-2B cell line was utilized to establish an EMT model in the present study. Generally, downregulated E-cadherin expression and upregulated N-cadherin, vimentin and α-SMA expression are reliable markers of EMT in

epithelial cells (4). In addition, increasing evidence reveals that the EMT process can increase cell migration and suppress apoptosis (27,28). As BEAS-2B cells are an epithelial cell line, they exhibit high basal expression of E-cadherin, which is an epithelial cell marker (29). After BEAS-2B cells were stimulated with 10 ng/ml TGF-β1 for 24 h, E-cadherin expression was significantly decreased and N-cadherin, vimentin and α-SMA expression was increased at the mRNA and protein levels. Moreover, compared with normal control airway tissues, AF tissues exhibited decreased E-cadherin expression, whereas TGF-β1, N-cadherin, vimentin and α-SMA expression was increased at the protein level. These findings indicated that TGF-β1 induced EMT, which is consistent with a previous study (30). Furthermore, overexpression of miR-423-5p promoted TGF-β1-induced EMT. Reciprocally, downregulation of miR-423-5p suppressed TGF-β1-induced EMT.

FOXP, which is a member of the forkhead transcription factor family, is involved in various cell processes, including migration, proliferation, ageing and the cell cycle, by its function in regulating transcription (31). FOXP consists of four members: FOXP1, FOXP2, FOXP3 and FOXP4. FOXP4 is ubiquitously expressed in different types of cells and has been studied in various types of disease (32). For instance, Tao *et al* (33) reported that 'FOXP4-AS1 promotes mantle cell lymphoma progression through the upregulation of NACC1 expression by inhibiting miR-423-5p'. Xiong *et al* (34) found that the 'circRNA ZNF609 functions as a competitive endogenous RNA to regulate FOXP4 expression by sponging miR-138-5p in renal carcinoma'. More notably, several studies have demonstrated that FOXP4 participates in the development of the EMT process (35,36). In the present study, FOXP4 was downregulated in AF tissues and BEAS-2B cells with TGF-β1-induced EMT and FOXP4 was also directly regulated by miR-423-5p. Furthermore, FOXP4 knockdown eliminated the miR-423-5p inhibitor-induced effect on TGF-β1-induced EMT. These results indicated that FOXP4 participated in AF via the EMT process and is a target gene of miR-423-5p.

Several studies have highlighted the critical role of the PI3K/AKT/mTOR pathway in the development of fibrosis in various organs, including the lungs, liver and myocardial tissue (37-39). When exogenous cytokines trigger cellular signals, the AKT signaling cascade is activated by receptors via PI3K phosphorylation, which immediately activates mTOR, resulting in the transcription of activation-related molecules (40). The results of the present study indicated that TGF-β1 increased the levels of p-PI3K, p-AKT and p-mTOR and that the miR-423-5p inhibitor decreased the levels of p-PI3K, p-AKT and p-mTOR. In addition, FOXP4 knockdown reversed the effect of the miR-423-5p inhibitor on the expression of p-PI3K, p-AKT and p-mTOR, showing that the miR-423-5p mimic promoted TGF-β1-induced EMT by targeting FOXP4 via PI3K/AKT/mTOR pathway activation.

However, the following limitations of the present study should be considered. Due to various factors, an *in vivo* experiment was not completed. Therefore, the effects of miR-423-5p in animal models of AF will be explored in the future. In addition, the present study did not investigate the effect of miR-423-5p overexpression on EMT (e.g., markers expression, migration and invasion) in BEAS-2B cells without TGF-β1 treatment because the aim was to investigate miR-423-5p function and its possible underlying mechanism in the EMT process of BEAS-2B cells. Unfortunately, the chest HRCT and bronchoscope images were lost due to the Coronavirus pandemic and attempts to find such data failed. Furthermore, caspase should be further detected to investigated cell apoptosis and rescue experiments should be done by overexpressing miR-423-5p or its target genes to make the results more solid. Additionally, it would be more effective to comprehensively estimate the cell transcriptome level by RNA-seq. Moreover, because a total of 10 AF scar tissue samples were collected from patients undergoing fiberoptic bronchoscopy biopsy via an electrocautery needle knife (VIO 300S; Erbe Elektromedizin GmbH) which led to destruction of normal airway tissue structure so the histopathological images could not be confirmed to originated from airway tissue in Fig. 1A. These defects will be remedied in the future.

In conclusion, the present study suggested that miR-423-5p promoted TGF-β1-induced EMT in AF by depressing FOXP4 expression and this effect may partly be attributed to the activation of the PI3K/AKT/mTOR pathway. Therefore, miR-423-5p inhibition may be a target for the prevention and treatment of AF.

Acknowledgements

Not applicable.

Funding

The present study was supported by the National Major Science and Technology Projects of China (grant no. 2018ZX10302302003).

Availability of data and materials

The datasets used and/or analyzed during the current study are available from the corresponding author on reasonable request.

Authors' contributions

YC and SG designed the experiments and revised the manuscript. YW analyzed the data and revised the manuscript. YC and XL performed the experiments and wrote the manuscript. YL, GH and XW analyzed the data. YC and SG confirm the authenticity of all the raw data. All authors read and approved the final manuscript.

Ethics approval and consent to participate

The First Affiliated Hospital of Chongqing Medical University Ethics Committee approved the present study (institutional approval number. 2020-147) and the research was performed in accordance with the Declaration of Helsinki.

Patient consent for publication

All subjects provided written informed consent.

Competing interests

The authors declare that they have no competing interests.

References

1. Rao W, Wang S, Duleba M, Niroula S, Goller K, Xie J, Mahalingam R, Neupane R, Liew AA, Vincent M, *et al*: Regenerative metaplastic clones in COPD lung drive inflammation and fibrosis. Cell 181: 848-864.e18, 2020.
2. Van Dyken SJ, Liang HE, Naikawadi RP, Woodruff PG, Wolters PJ, Erle DJ and Locksley RM: Spontaneous chitin accumulation in airways and age-related fibrotic lung disease. Cell 169: 497-509.e13, 2017.
3. Swatek AM, Lynch TJ, Crooke AK, Anderson PJ, Tyler SR, Brooks L, Ivanovic M, Klesney-Tait JA, Eberlein M, Pena T, *et al*: Depletion of airway submucosal glands and $TP63^{+}KRT5^{+}$ basal cells in obliterative bronchiolitis. Am J Respir Crit Care Med 197: 1045-1057, 2018.
4. Tian B, Hosoki K, Liu Z, Yang J, Zhao Y, Sun H, Zhou J, Rytting E, Kaphalia L, Calhoun WJ, *et al*: Mucosal bromodomain-containing protein 4 mediates aeroallergen-induced inflammation and remodeling. J Allergy Clin Immunol 143: 1380-1394.e9, 2019.
5. Di Campli MP, Azouz A, Assabban A, Scaillet J, Splittgerber M, Van Keymeulen A, Libert F, Remmelink M, Le Moine A, Lemaitre P and Goriely S: The mononuclear phagocyte system contributes to fibrosis in post-transplant obliterans bronchiolitis. Eur Respir J 57: 2000344, 2021.
6. Yang J, Tian B, Sun H, Garofalo RP and Brasier AR: Epigenetic silencing of IRF1 dysregulates type III interferon responses to respiratory virus infection in epithelial to mesenchymal transition. Nat Microbiol 2: 17086, 2017.
7. Su J, Morgani SM, David CJ, Wang Q, Er EE, Huang YH, Basnet H, Zou Y, Shu W, Soni RK, *et al*: TGF-β orchestrates fibrogenic and developmental EMTs via the RAS effector RREB1. Nature 577: 566-571, 2020.
8. Piera-Velazquez S and Jimenez SA: Endothelial to mesenchymal transition: Role in physiology and in the pathogenesis of human diseases. Physiol Rev 99: 1281-1324, 2019.
9. Yates LA, Norbury CJ and Gilbert RJ: The long and short of microRNA. Cell 153: 516-519, 2013.
10. Jones D: Setbacks shadow microRNA therapies in the clinic. Nat Biotechnol 36: 909-910, 2018.
11. Yang ZC, Qu ZH, Yi MJ, Shan YC, Ran N, Xu L and Liu XJ: MiR-448-5p inhibits TGF-β1-induced epithelial-mesenchymal transition and pulmonary fibrosis by targeting Six1 in asthma. J Cell Physiol 234: 8804-8814, 2019.
12. Li J, Pan C, Tang C, Tan W, Zhang W and Guan J: MiR-184 targets TP63 to block idiopathic pulmonary fibrosis by inhibiting proliferation and epithelial-mesenchymal transition of airway epithelial cells. Lab Invest 101: 142-154, 2021.
13. Hou Y, Zhang Y, Lin S, Yu Y, Yang L, Li L and Wang W: Protective mechanism of apigenin in diabetic nephropathy is related to its regulation of miR-423-5P-USF2 axis. Am J Transl Res 13: 2006-2020, 2021.
14. Livak KJ and Schmittgen TD: Analysis of relative gene expression data using real-time quantitative PCR and the 2(-delta delta C(T)) method. Methods 25: 402-408, 2001.
15. Michalik M, Wójcik-Pszczoła K, Paw M, Wnuk D, Koczurkiewicz P, Sanak M, Pękala E and Madeja Z: Fibroblast-to-myofibroblast transition in bronchial asthma. Cell Mol Life Sci 75: 3943-3961, 2018.
16. Zaiss DMW: Amphiregulin as a driver of tissue fibrosis. Am J Transplant 20: 631-632, 2020.
17. Zhao Y, Shen X, Tang T and Wu CI: Weak regulation of many targets is cumulatively powerful-an evolutionary perspective on microRNA functionality. Mol Biol Evol 34: 3041-3046, 2017.
18. Guiot J, Cambier M, Boeckx A, Henket M, Nivelles O, Gester F, Louis E, Malaise M, Dequiedt F, Louis R, *et al*: Macrophage-derived exosomes attenuate fibrosis in airway epithelial cells through delivery of antifibrotic miR-142-3p. Thorax 75: 870-881, 2020.
19. Pommier A, Varilh J, Bleuse S, Delétang K, Bonini J, Bergougnoux A, Brochiero E, Koenig M, Claustres M and Taulan-Cadars M: miRNA repertoires of cystic fibrosis ex vivo models highlight miR-181a and miR-101 that regulate WISP1 expression. J Pathol 253: 186-197, 2021.
20. Liu Y, Bi X, Xiong J, Han W, Xiao T, Xu X, Yang K, Liu C, Jiang W, He T, *et al*: MicroRNA-34a Promotes renal fibrosis by downregulation of klotho in tubular epithelial cells. Mol Ther 27: 1051-1065, 2019.
21. Song L, Chen TY, Zhao XJ, Xu Q, Jiao RQ, Li JM and Kong LD: Pterostilbene prevents hepatocyte epithelial-mesenchymal transition in fructose-induced liver fibrosis through suppressing miR-34a/Sirt1/p53 and TGF-β1/Smads signalling. Br J Pharmacol 176: 1619-1634, 2019.
22. Yeh HW, Hsu EC, Lee SS, Lang YD, Lin YC, Chang CY, Lee SY, Gu DL, Shih JH, Ho CM, *et al*: PSPC1 mediates TGF-β1 autocrine signalling and Smad2/3 target switching to promote EMT, stemness and metastasis. Nat Cell Biol 20: 479-491, 2018.
23. Sun Y, Shi Z, Liu B, Li X, Li G, Yang F and Tang H: YKL-40 mediates airway remodeling in asthma via activating FAK and MAPK signaling pathway. Cell Cycle 19: 1378-1390, 2020.
24. Wang J, Tian X, Zhang J, Tan L, Ouyang N, Jia B, Chen C, Ge C and Li J: Postchronic single-walled carbon nanotube exposure causes irreversible malignant transformation of human bronchial epithelial cells through DNA methylation changes. ACS Nano 15: 7094-7104, 2021.
25. Benedikter BJ, Bouwman FG, Heinzmann ACA, Vajen T, Mariman EC, Wouters EFM, Savelkoul PHM, Koenen RR, Rohde GGU, van Oerle R, *et al*: Proteomic analysis reveals procoagulant properties of cigarette smoke-induced extracellular vesicles. J Extracell Vesicles 8: 1585163, 2019.
26. Sundar IK, Li D and Rahman I: Small RNA-sequence analysis of plasma-derived extracellular vesicle miRNAs in smokers and patients with chronic obstructive pulmonary disease as circulating biomarkers. J Extracell Vesicles 8: 1684816, 2019.
27. Gao Y, Shang S, Guo S, Li X, Zhou H, Liu H, Sun Y, Wang J, Wang P, Zhi H, *et al*: Lnc2Cancer 3.0: An updated resource for experimentally supported lncRNA/circRNA cancer associations and web tools based on RNA-seq and scRNA-seq data. Nucleic Acids Res 49(D1): D1251-D1258, 2021.
28. Serresi M, Kertalli S, Li L, Schmitt MJ, Dramaretska Y, Wierikx J, Hulsman D and Gargiulo G: Functional antagonism of chromatin modulators regulates epithelial-mesenchymal transition. Sci Adv 7: eabd7974, 2021.
29. Bernstein DI, Lummus ZL, Kesavalu B, Yao J, Kottyan L, Miller D, Cartier A, Cruz MJ, Lemiere C, Muñoz X, *et al*: Genetic variants with gene regulatory effects are associated with diisocyanate-induced asthma. J Allergy Clin Immunol 142: 959-969, 2018.
30. Zhang X, Liu L, Deng X, Li D, Cai H, Ma Y, Jia C, Wu B, Fan Y and Lv Z: MicroRNA 483-3p targets Pard3 to potentiate TGF-β1-induced cell migration, invasion and epithelial-mesenchymal transition in anaplastic thyroid cancer cells. Oncogene 38: 699-715, 2019.
31. Kim JH, Hwang J, Jung JH, Lee HJ, Lee DY and Kim SH: Molecular networks of FOXP family: Dual biologic functions, interplay with other molecules and clinical implications in cancer progression. Mol Cancer 18: 180, 2019.
32. Snijders Blok L, Vino A, den Hoed J, Underhill HR, Monteil D, Li H, Reynoso Santos FJ, Chung WK, Amaral MD, Schnur RE, *et al*: Heterozygous variants that disturb the transcriptional repressor activity of FOXP4 cause a developmental disorder with speech/language delays and multiple congenital abnormalities. Genet Med 23: 534-542, 2021.
33. Tao HF, Shen JX, Hou ZW, Chen SY, Su YZ and Fang JL: lncRNA FOXP4-AS1 predicts poor prognosis and accelerates the progression of mantle cell lymphoma through the miR-423-5p/NACC1 pathway. Oncol Rep 45: 469-480, 2021.
34. Xiong Y, Zhang J and Song C: CircRNA ZNF609 functions as a competitive endogenous RNA to regulate FOXP4 expression by sponging miR-138-5p in renal carcinoma. J Cell Physiol 234: 10646-10654, 2019.
35. Rajarajan D, Selvarajan S, Charan Raja MR, Kar Mahapatra S and Kasiappan R: Genome-wide analysis reveals miR-3184-5p and miR-181c-3p as a critical regulator for adipocytes-associated breast cancer. J Cell Physiol 234: 17959-17974, 2019.
36. E C, Yang J, Li H and Li C: LncRNA LOC105372579 promotes proliferation and epithelial-mesenchymal transition in hepatocellular carcinoma via activating miR-4316/FOXP4 signaling. Cancer Manag Res 11: 2871-2879, 2019.
37. Han B, Chu C, Su X, Zhang N, Zhou L, Zhang M, Yang S, Shi L, Zhao B, Niu Y and Zhang R: N^{6}-methyladenosine-dependent primary microRNA-126 processing activated PI3K-AKT-mTOR pathway drove the development of pulmonary fibrosis induced by nanoscale carbon black particles in rats. Nanotoxicology 14: 1-20, 2020.

38. Kong D, Zhang Z, Chen L, Huang W, Zhang F, Wang L, Wang Y, Cao P and Zheng S: Curcumin blunts epithelial-mesenchymal transition of hepatocytes to alleviate hepatic fibrosis through regulating oxidative stress and autophagy. Redox Biol 36: 101600, 2020.
39. Liang M, Lv J, Jiang Z, He H, Chen C, Xiong Y, Zhu X, Xue Y, Yu Y, Yang S, *et al*: Promotion of myofibroblast differentiation and tissue fibrosis by the leukotriene B_4 -leukotriene B_4 receptor axis in systemic sclerosis. Arthritis Rheumatol 72: 1013-1025, 2020.
40. Janku F, Yap TA and Meric-Bernstam F: Targeting the PI3K pathway in cancer: Are we making headway. Nat Rev Clin Oncol 15: 273-291, 2018.